Environmental Science & Technology Letters

Letter

Cite This: Environ. Sci. Technol. Lett. 2019, 6, 520−524

pubs.acs.org/journal/estlcu

Autoxidation of Limonene Emitted in a University Art Museum

Demetrios Pagonis,[†,‡] Lucas B. Algrim,[†,‡] Derek J. Price,[†,‡] Douglas A. Day,[†,‡] Anne V. Handschy,[†,‡] Harald Stark,[†,‡,§] Shelly L. Miller,[∥] Joost A. de Gouw,[†,‡] Jose L. Jimenez,[†,‡] and Paul J. Ziemann*[,†,‡]

[†]Cooperative Institute for Research in Environmental Sciences (CIRES), University of Colorado, Boulder, Colorado 80309, United States

[‡]Department of Chemistry, University of Colorado, Boulder, Colorado 80309, United States

[§]Aerodyne Research, Inc., Billerica, Massachusetts 01821, United States

[∥]Department of Mechanical Engineering, University of Colorado, Boulder, Colorado 80309, United States

Supporting Information

ABSTRACT: The lifetime of alkylperoxy radicals ($RO_2^•$) formed in the oxidation of volatile organic compounds (VOCs) is a key determinant of reaction mechanisms and products. When $RO_2^•$ radical lifetimes are long, autoxidation reactions can form highly oxidized multifunctional compounds (HOMs) that are efficient at forming secondary organic aerosol (SOA). We measured the formation of HOMs resulting from the O_3-initiated autoxidation of limonene emitted inside the University of Colorado Art Museum. Conditions inside the museum favored autoxidation for most of the 6-week study, indicating that autoxidation is prevalent indoors in the absence of an indoor combustion source of nitrogen oxide (NO). A box model of the museum was used with measurements of VOCs, O_3, and NO_x and air exchange to estimate HOM and SOA yields and to model the limonene oxidation rate. The HOM molar yield of 11% agrees well with the results of laboratory studies of limonene autoxidation, and the SOA mass yield of 47 ± 8% indicates that limonene autoxidation efficiently forms SOA indoors.

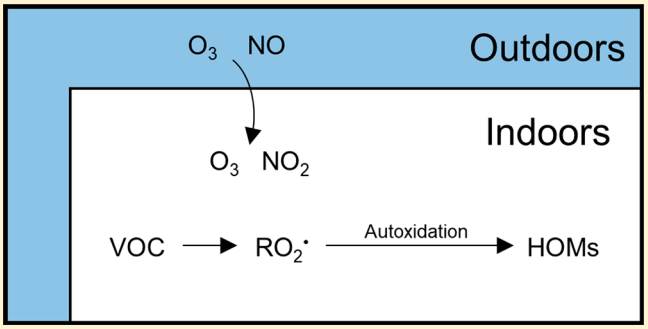

INTRODUCTION

On average, Americans spend 90% of their time indoors, where they are exposed to products of reactions that occur in the indoor environment.[1] Indoor oxidation of volatile organic compounds (VOCs) can lead to the formation of low-volatility products that condense to form secondary organic aerosol (SOA), measurably increasing the mass concentration of submicrometer particulate matter.[2−4] Whereas reactions of alkenes with O_3 are known to be important in this regard,[5] reactions initiated by OH or NO_3 radicals (the other major atmospheric oxidants) are expected to be less significant in most indoor environments.[5−9] Most VOC oxidation reactions proceed through the formation of alkylperoxy radicals ($RO_2^•$), which, depending on conditions, react with NO, HO_2, or $RO_2^•$ radicals or isomerize.[10−12] The products produced by each of these pathways are chemically different, and these differences can impact the amount and properties of SOA formed. In polluted air, where emissions of NO from combustion are substantial, $RO_2^•$ radicals react primarily with NO to form either alkyl nitrates or alkoxy radicals ($RO^•$) and NO_2, with the $RO^•$ radicals reacting further to form a variety of products that typically contain carbonyl, hydroxyl, and nitrate groups. In clean air, isomerization of $RO_2^•$ radicals and their reactions with HO_2 or $RO_2^•$ radicals become competitive with and can dominate over NO reactions, typically leading to products containing carbonyl, hydroxyl, carboxyl, and peroxide groups. In particular, $RO_2^•$ radical isomerization, which involves an H-shift and is a key pathway in so-called "autoxidation", has attracted much attention in recent years because it can lead to the formation of highly oxidized multifunctional compounds (HOMs) that are efficient in forming SOA.[13] It has been shown that HOMs can comprise the majority of SOA produced in pristine forested environments,[13] and their contribution to urban SOA is expected to grow in areas where NO concentrations are decreasing due to air quality regulations.[14]

In light of these new developments in our understanding of atmospheric VOC oxidation and SOA formation, we have begun to explore the potential role of autoxidation in indoor environments. There, NO concentrations are determined by infiltration of outdoor air and by indoor emissions from

Received: July 13, 2019
Revised: August 16, 2019
Accepted: August 16, 2019
Published: August 16, 2019

DOI: 10.1021/acs.estlett.9b00425
Environ. Sci. Technol. Lett. 2019, 6, 520−524

combustion sources.[5] Ozone is present in significant concentrations under most conditions due to infiltration of outdoor air and is also emitted from air cleaners, printers, and other devices. Because O_3 rapidly titrates NO to NO_2, and photolysis of NO_2 is limited by the absence of strong light, in the absence of indoor combustion, conditions favoring autoxidation are expected to be more common indoors than outdoors. Additionally, VOC emissions indoors often occur as transient events due to cooking, cleaning, eating, and other human activities. Here, we simulated one such event by peeling an orange in the University of Colorado Art Museum, with the amount of limonene emitted being comparable to that of VOCs typically emitted by other activities. An advantage of studying this particular event is that an orange emits primarily a single monoterpene (limonene) instead of a complex mixture of VOCs.[9,15−18] We then employed real time mass spectrometry to clearly identify gas-phase HOMs formed from limonene ozonolysis, demonstrating that indoor $RO_2^•$ radical lifetimes can be sufficiently long to allow autoxidation to occur. We also measured the yields of HOMs and SOA, showing that autoxidation can significantly increase the concentrations of these gas-phase reaction products as well as aerosol mass.

EXPERIMENTAL SECTION

Art Museum Site. The Art Museum Study of Indoor Chemistry (ARTISTIC) was conducted at the University of Colorado Art Museum over 6 weeks, beginning in April 2017. The 6000 m^3 building has a constant air change rate of 0.8 h^{-1} with outside air, and measurements were conducted in a 780 m^3 gallery with a constant air exchange rate of 10 h^{-1}. The supply air delivered to the gallery by the air handler consisted of 90% recirculated air and 10% outdoor air (Figure S1).

Measurements and Instrumentation. Concentrations of VOCs in the museum were measured using a quadrupole proton-transfer-reaction mass spectrometer (PTR-MS),[19] and HOMs were measured using a high-resolution time-of-flight nitrate adduct chemical ionization mass spectrometer (NO_3-CIMS).[20] Compounds detected by the NO_3-CIMS were quantified by assuming they cluster with nitrate anions at the collision limit[13,21] and that 35% of HOMs are lost irreversibly following diffusion to the walls of the inlet (assuming laminar flow and unit uptake coefficient).[22] Aerosol size distributions and mass concentrations were measured over the range of 15−600 nm with a TSI scanning mobility particle sizer (SMPS) (model 3080 differential mobility analyzer and model 3775 condensation particle counter). Ozone and NO concentrations were measured with Thermo 49i and 42i-TL analyzers. Sampling and calibration details are presented in ref 9. Details of background aerosol and limonene SOA density estimates and use with SMPS measurements are presented in the Supporting Information.

Art Museum Model. The box model used to describe the chemistry, transport, and deposition of compounds inside the museum is described in ref 9 and briefly summarized here. It is equivalent to a two-compartment completely mixed flow reactor model,[23] where the two compartments used to describe the museum are the gallery where measurements were taken and the supply air combined with the air from the rest of the building, each of which is assumed to be well mixed (Figure S1). The model employs measurements of VOCs, O_3, and NO_x in the gallery and supply air and the air exchange rate to estimate indoor concentrations of OH radicals and NO_3 radicals, which are produced from reactions of O_3 with alkenes and NO_2, respectively. The model includes photolysis reactions, but because the galleries are windowless and light with wavelengths <400 nm is essentially eliminated by ultraviolet filters installed on the gallery light fixtures, these reactions were negligibly slow. For example, on the basis of spectral measurements and calculations described previously,[9] the lifetime of NO_2 with respect to photolysis is ∼25 days (j_{NO_2} = 4.6 × 10^{-7} s^{-1}), so its overall lifetime is ∼1.3 h due to air exchange.

RESULTS AND DISCUSSION

Indoor HOM Production. We measured the formation of HOMs indoors following a perturbation experiment in which a navel orange was peeled inside the museum, releasing monoterpenes that were quantified by the PTR-MS. Because measurements by Arey et al.[24] indicated that >90% of the mass of monoterpenes emitted from a navel orange are limonene and the PTR-MS does not separate monoterpenes, we assumed that those emitted in the museum were entirely this compound. The increase in the concentration of limonene was 2.3 ppb (corresponding to 77 mg emitted into the entire building) and occurred while the gallery O_3, NO, and NO_2 concentrations were 5.9, 0.055, and 10.4 ppb, respectively. The NO concentrations in the museum were thus sufficiently low to allow for O_3-initiated autoxidation, which has been observed for NO concentrations of ≤800 ppt.[25] The average NO_3-CIMS mass spectra during the hour preceding and the hour following the event are presented in Figure 1, clearly showing that the signal intensity of peaks associated with a number of compounds increased following the release of limonene. The high O:C ratios of molecular formulas assigned to those peaks (0.4−1.1) are characteristic of HOMs. We attribute the similarity in peak patterns of newly formed HOMs and background to weak off-gassing of limonene from the orange as it sat in the room before being peeled, although no measurable enhancement above the 0.4 ppb monoterpene background was observed. Background mass spectra recorded on other days during the study did not exhibit the same pattern (Figure S3), so we do not attribute these HOMs to oxidation of monoterpenes from personal care or cleaning products. The nitrogen present in some peaks could come from limonene + NO_3 radical reactions, but the analysis discussed below indicates that the latter reactions made negligible contributions to HOM formation. Thus, the nitrogen in the HOMs is likely due to radical chain-terminating formation of nitrate groups by the $RO_2^•$ + NO reaction. A list of assigned molecular formulas

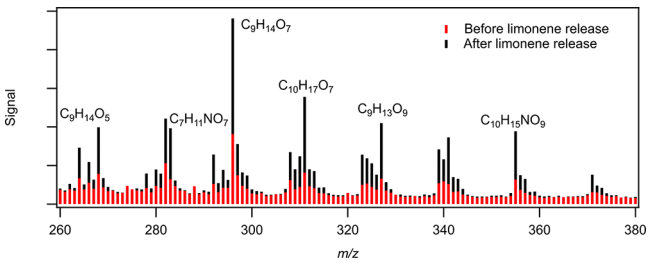

Figure 1. NO_3-CIMS mass spectra averaged for the hour before and the hour after limonene was emitted into the museum by peeling an orange. The elemental formulas above some peaks are the assigned elemental formula minus the nitrate ion (NO_3^-).

DOI: 10.1021/acs.estlett.9b00425
Environ. Sci. Technol. Lett. 2019, 6, 520−524

for peaks with intensities that increased following limonene emission is presented in Table S1. Example peak fits of identified ions are presented in Figure S4.

Limonene Oxidation Rate and HOM Yields. We evaluated the model predictions of VOC oxidation rate using the measured loss rate of limonene determined from the PTR-MS time series of characteristic ions at m/z 81 and 137.[26] As shown in Figure 2A, the time scale for limonene removal

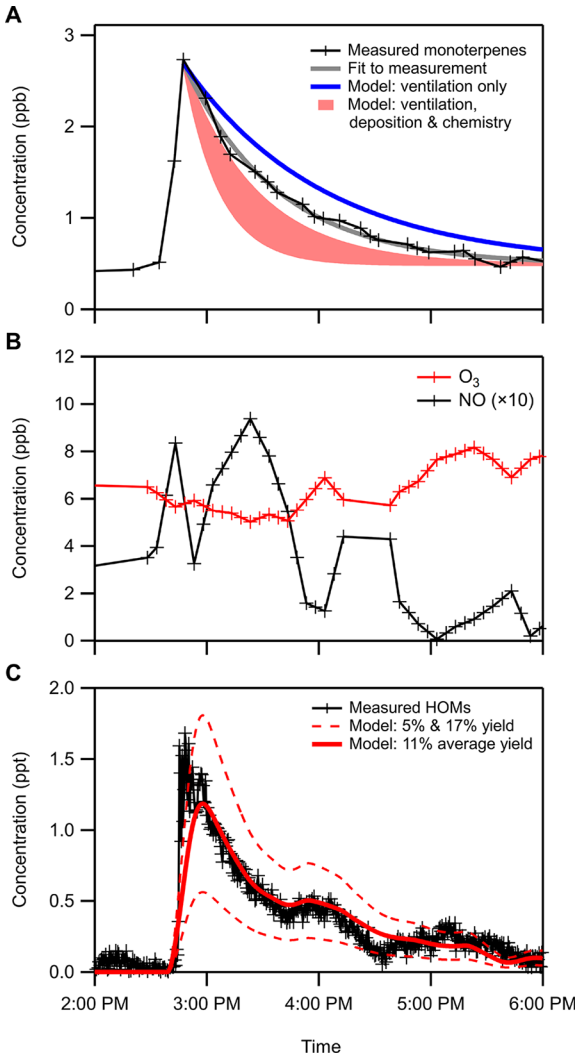

Figure 2. (A) Measured and modeled time series of the limonene component of monoterpenes in the museum following emission from a peeled orange, where the model includes removal by ventilation alone or by ventilation, deposition, and chemistry. (B) Measured O_3 and NO (scaled 10×) concentrations in the museum following limonene emission. (C) Measured and modeled concentrations of highly oxidized multifunctional compounds (HOMs) produced from limonene ozonolysis in the museum, where the model assumes yields of 5%, 17%, or 11% (average).

following emission was 0.86 ± 0.04 h, faster than the 1.25 h time scale for indoor−outdoor air exchange for unreactive gases such as CO_2.[9] To model the total removal time scale for limonene, we considered removal by gas-phase reactions and uptake by surfaces in addition to air exchange. Using O_3 measurements and model estimates of radical concentrations in the museum ([OH] = 10^5 molecules cm^{-3}; [NO_3] = 3×10^6 molecules cm^{-3}),[9] the limonene oxidation time scale was 3.3 h (τ_{O_3} = 8.3 h, τ_{OH} = 17 h, and τ_{NO_3} = 7.7 h), and using the relationship developed by Pagonis et al.[9] between deposition rates in the museum and the saturation vapor concentrations (C^*)[27] and Henry's law constants (K_H) calculated using structure−activity relationships,[28,29] we estimate a deposition time scale for limonene between 0.5 and 2.4 h (limonene C^* = 2×10^7 μg m^{-3} and K_H = 2×10^{-2} M atm^{-1}). When ventilation, oxidation, and deposition occur in parallel, the predicted range of time scales for removal of limonene from the museum is 0.32−0.65 h. The upper end of this range (where deposition is slowest) is sufficiently close to the measured removal time scale of 0.86 h to give confidence that the model provides a reasonable description of the processes influencing the limonene time series. Additionally, the C^* of limonene is roughly equal to that of the most volatile compound for which deposition was observed,[9] and given the uncertainties in SIMPOL.1[28] vapor pressures used to calculate C^* values, it is possible that limonene deposits more slowly than the range reported here.

As a result of the reaction of limonene with O_3, the concentrations of HOMs in the gallery measured by the NO_3-CIMS increased in parallel with the limonene concentration. Figure 2C shows the time series of HOMs formed from limonene oxidation, calculated by summing the time series of compounds detected at m/z ≥250 that increased by ≥3σ following the release of limonene (where σ is the standard deviation in the ion signal in the hour preceding limonene release). Comparison to limonene oxidation rates predicted by the model indicates that ≥96% of the HOMs were produced through ozonolysis. The complete analysis of the relative contributions of different oxidants to HOM formation is presented in the Supporting Information. Published HOM yields for limonene ozonolysis are 5.3% and 17%,[13,30] and model predictions using each of these yields, their average, and the amount of limonene that reacted with O_3 are shown alongside our measurements of indoor HOMs in Figure 2C. The modeled HOMs peak later than the measurements because of the slower sampling rate of the PTR-MS. The average HOM yield of 11% results in a modeled HOM concentration in good agreement with measurements. We also assumed the HOMs had sufficiently low volatility that they were quantitatively (99%) removed from the museum supply air by deposition to surfaces inside the ventilation system (τ_{dep} < 1.6 min[9]), and thus, the concentration brought into the gallery was zero. Because HOMs are also expected to partition entirely to the particle phase,[13] we included a condensational sink of τ_{cs} = 13 min quantified from the SMPS aerosol size distribution as described in the Supporting Information.

SOA Formation. Because HOMs contribute significantly to particulate matter in pristine outdoor environments[13] and orange peeling is known to form SOA indoors,[31,32] we evaluated the impact of HOM formation on aerosol mass inside the museum. As shown in Figure 3, the aerosol mass concentration measured by the SMPS increased by 0.3 μg m^{-3} in the hour following limonene emission. Adding SOA formation to the model of Pagonis et al.,[9] we estimate SOA yields for limonene of 47 ± 8% and 28 ± 9% for reactions with O_3 and NO_3 radicals, respectively. Details of the modeling and error analysis are presented in the Supporting Information. Because this analysis does not account for the aerosol filters in the HVAC system (discussed in the Supporting Information), our estimated yields are lower bounds. The SOA yield

DOI: 10.1021/acs.estlett.9b00425
Environ. Sci. Technol. Lett. 2019, 6, 520−524

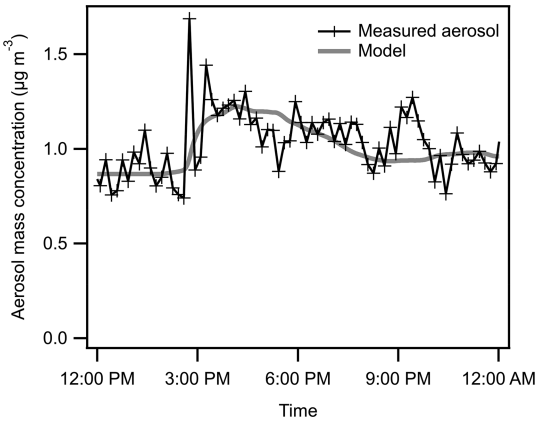

Figure 3. Comparison of aerosol mass concentration inside the museum following emission of limonene from a peeled orange, measured by the SMPS and estimated using a box model that includes SOA formation from limonene ozonolysis.

of 47% estimated for the O_3 reaction is ~2 times the yield of 24% measured by Claflin et al.[33] for the reaction of α-pinene under autoxidation conditions at 55% relative humidity and ~4 times the yield of 11% estimated by a parametrization developed for limonene oxidation from chamber studies not conducted under autoxidation conditions.[34] Because SOA yields in outdoor environments can be dominated by HOMs,[13] these results suggest that HOMs can also be a significant source of indoor SOA.

Implications for Indoor Oxidation Mechanisms. The observed HOM production in the gallery shows that autoxidation is a significant fate for $RO_2^\bullet$ radicals indoors when NO concentrations are low. Using measurements of NO in the museum and an $RO_2^\bullet$ + NO reaction rate constant of 9×10^{-12} cm^3 $molecule^{-1}$ s^{-1},[35] we estimate a bimolecular reaction lifetime of $RO_2^\bullet$ radicals of >1 s for 99% of the ARTISTIC campaign. Comparing this to the $RO_2^\bullet$ radical isomerization lifetime of 0.25 s measured for ring-opened alkylperoxy radicals formed from OH radical-initiated reactions of α-pinene[36] indicates that bimolecular $RO_2^\bullet$ radical reactions were sufficiently slow to allow autoxidation to proceed during most of the study. While NO concentrations in human breath are between 5 and 50 ppb,[37] those emissions were too small to reduce the $RO_2^\bullet$ lifetime below 10 s, as shown in Figure S5.

In this study, rapid titration of NO by excess O_3 (τ = 6.6 min), low rates of NO production by NO_2 photolysis (τ = 25 days), and the absence of significant indoor NO emissions created an environment that favored low-NO_x chemistry initiated by O_3, where $RO_2^\bullet$ radical intermediates reacted with HO_2 and $RO_2^\bullet$ radicals and by autoxidation. Because conditions with some O_3 and a low level of NO should be pervasive indoors, due to O_3 infiltration and limited NO in the absence of indoor combustion,[38] continued research on outdoor VOC autoxidation and subsequent SOA formation will also be broadly applicable to indoor air chemistry. However, in environments in which O_3 is titrated by excess NO_x, such as buildings with indoor combustion sources,[38] high-NO_x chemistry is likely dominant. Oxidation is then initiated primarily by reaction with OH radicals, and most $RO_2^\bullet$ radicals react with NO. As in outdoor air, defining the oxidation regime of a particular indoor environment allows for placement of better constraints when modeling oxidation rates, reaction products, and SOA yields.

■ ASSOCIATED CONTENT

Supporting Information

The Supporting Information is available free of charge on the ACS Publications website at DOI: 10.1021/acs.estlett.9b00425.

Details of particle density and molecular weight estimates; a schematic of the box model; calculations of the relative contribution of O_3, NO_3, and OH to HOM formation; Monte Carlo error analysis of fit parameters; ambient NO_3-CIMS spectra used to evaluate background HOMs; a table of detected NO_3-CIMS m/z values and assignments; example high-resolution peak fits of assigned m/z values; calculation of the aerosol condensation sink; a discussion of the impacts of aerosol filters on SOA yields in the museum; and calculations of NO emissions by human breath (PDF)

■ AUTHOR INFORMATION

Corresponding Author

*E-mail: paul.ziemann@colorado.edu.

ORCID

Demetrios Pagonis: 0000-0002-0441-2614
Derek J. Price: 0000-0003-3693-1475
Douglas A. Day: 0000-0003-3213-4233
Harald Stark: 0000-0002-0731-1202
Joost A. de Gouw: 0000-0002-0385-1826
Jose L. Jimenez: 0000-0001-6203-1847
Paul J. Ziemann: 0000-0001-7419-0044

Notes

The authors declare no competing financial interest.

■ ACKNOWLEDGMENTS

The authors thank the Alfred P. Sloan Foundation (Grant G-2016-7173) for funding and Stephen Martonis, Pedro Caceres, and Sandra Firmin at the University of Colorado Boulder Art Museum for their help during the study.

■ REFERENCES

(1) Klepeis, N. E.; Nelson, W. C.; Ott, W. R.; Robinson, J. P.; Tsang, A. M.; Switzer, P.; Behar, J. V.; Hern, S. C.; Engelmann, W. H. The national human activity pattern survey (NHAPS). A resource for assessing exposure to environmental pollutants. *J. Exposure Sci. Environ. Epidemiol.* **2001**, *11*, 231−252.

(2) Weschler, C. J.; Shields, H. C. Indoor ozone/terpene reactions as a source of indoor particles. *Atmos. Environ.* **1999**, *33*, 2301−2312.

(3) Long, C. M.; Suh, H. H.; Koutrakis, P. Characterization of indoor particle sources using continuous mass and size monitors. *J. Air Waste Manage. Assoc.* **2000**, *50*, 1236−1250.

(4) Wainman, T.; Zhang, J.; Weschler, C. J.; Lioy, P. J. Ozone and limonene in indoor air: A source of submicron particle exposure. *Environ. Health Perspect.* **2000**, *108*, 1139−1145.

(5) Weschler, C. J.; Carslaw, N. Indoor chemistry. *Environ. Sci. Technol.* **2018**, *52*, 2419−2428.

(6) Gomez Alvarez, E.; Amedro, D.; Afif, C.; Gligorovski, S.; Schoemaecker, C.; Fittschen, C.; Doussin, J. F.; Wortham, H. Unexpectedly high indoor hydroxyl radical concentrations associated with nitrous acid. *Proc. Natl. Acad. Sci. U. S. A.* **2013**, *110*, 13294−13299.

(7) Waring, M. S.; Wells, J. R. Volatile organic compound conversion by ozone, hydroxyl radicals, and nitrate radicals in residential indoor air: Magnitudes and impacts of oxidant sources. *Atmos. Environ.* **2015**, *106*, 382−391.

DOI: 10.1021/acs.estlett.9b00425
Environ. Sci. Technol. Lett. 2019, 6, 520−524

(8) Arata, C.; Zarzana, K. J.; Misztal, P. K.; Liu, Y.; Brown, S. S.; Nazaroff, W. W.; Goldstein, A. H. Measurement of NO_3 and N_2O_5 in a residential kitchen. *Environ. Sci. Technol. Lett.* **2018**, *5*, 595−599.
(9) Pagonis, D.; Price, D. J.; Algrim, L. B.; Day, D. A.; Handschy, A. H.; Stark, H.; Miller, S. L.; de Gouw, J.; Jimenez, J. L.; Ziemann, P. J. Time resolved measurements of indoor chemical emissions, deposition, and reactions in a university art museum. *Environ. Sci. Technol.* **2019**, *53*, 4794−4802.
(10) Orlando, J. J.; Tyndall, G. S. Laboratory studies of organic peroxy radical chemistry: an overview with emphasis on recent issues of atmospheric significance. *Chem. Soc. Rev.* **2012**, *41*, 6294−6317.
(11) Ziemann, P. J.; Atkinson, R. Kinetics, products, and mechanisms of secondary organic aerosol formation. *Chem. Soc. Rev.* **2012**, *41*, 6582−6605.
(12) Crounse, J. D.; Nielsen, L. B.; Jorgensen, S.; Kjaergaard, H. G.; Wennberg, P. O. Autoxidation of organic compounds in the atmosphere. *J. Phys. Chem. Lett.* **2013**, *4*, 3513−3520.
(13) Ehn, M.; Thornton, J. A.; Kleist, E.; Sipilä, M.; Junninen, H.; Pullinen, I.; Springer, M.; Rubach, F.; Tillmann, R.; Lee, B.; Lopez-Hilfiker, F.; Andres, S.; Acir, I. H.; Rissanen, M.; Jokinen, T.; Schobesberger, S.; Kangasluoma, J.; Kontkanen, J.; Nieminen, T.; Kurtén, T.; Nielsen, L. B.; Jørgensen, S.; Kjaergaard, H. G.; Canagaratna, M.; Maso, M. D.; Berndt, T.; Petäjä, T.; Wahner, A.; Kerminen, V. M.; Kulmala, M.; Worsnop, D. R.; Wildt, J.; Mentel, T. F. A large source of low-volatility secondary organic aerosol. *Nature* **2014**, *506*, 476−479.
(14) Praske, E.; Otkjær, R. V.; Crounse, J. D.; Hethcox, J. C.; Stoltz, B. M.; Kjaergaard, H. G.; Wennberg, P. O. Atmospheric autoxidation is increasingly important in urban and suburban North America. *Proc. Natl. Acad. Sci. U. S. A.* **2018**, *115*, 64−69.
(15) Schripp, T.; Etienne, S.; Fauck, C.; Fuhrmann, F.; Mark, L.; Salthammer, T. Application of proton-transfer-reaction-mass-spectrometry for indoor air quality research. *Indoor Air* **2014**, *24*, 178−189.
(16) Ampollini, L.; Katz, E. F.; Bourne, S.; Tian, Y.; Novoselac, A.; Goldstein, A. H.; Lucic, G.; Waring, M. S.; DeCarlo, P. Observations and contributions of real-time indoor ammonia concentrations during HOMEChem. *Environ. Sci. Technol.* **2019**, *53*, 8591.
(17) Duncan, S. M.; Tomaz, S.; Morrison, G.; Webb, M.; Atkin, J.; Surratt, J. D.; Turpin, B. J. Dynamics of residential water-soluble organic gases: Insights into sources and sinks. *Environ. Sci. Technol.* **2019**, *53*, 1812−1821.
(18) Liu, Y.; Misztal, P. K.; Xiong, J.; Tian, Y.; Arata, C.; Weber, R. J.; Nazaroff, W. W.; Goldstein, A. H. Characterizing sources and emissions of volatile organic compounds in a northern California residence using space- and time-resolved measurements. *Indoor Air* **2019**, *29*, 630−644.
(19) de Gouw, J.; Warneke, C. Measurements of volatile organic compounds in the earth's atmosphere using proton-transfer reaction mass spectrometry. *Mass Spectrom. Rev.* **2007**, *26*, 223−257.
(20) Jokinen, T.; Sipila, M.; Junninen, H.; Ehn, M.; Lonn, G.; Hakala, J.; Petaja, T.; Mauldin, R. L., III; Kulmala, M.; Worsnop, D. R. Atmospheric sulphuric acid and neutral cluster measurements using CI-APi-TOF. *Atmos. Chem. Phys.* **2012**, *12*, 4117−4125.
(21) Krechmer, J. E.; Coggon, M. M.; Massoli, P.; Nguyen, T. B.; Crounse, J. D.; Hu, W.; Day, D. A.; Tyndall, G. S.; Henze, D. K.; Rivera-Rios, J. C.; Nowak, J. B.; Kimmel, J. R.; Mauldin, R. L., III; Stark, H.; Jayne, J. T.; Sipila, M.; Junninen, H.; St. Clair, J. M.; Zhang, X.; Feiner, P. A.; Zhang, L.; Miller, D. O.; Brune, W. H.; Keutsch, F. N.; Wennberg, P. O.; Seinfeld, J. H.; Worsnop, D. R.; Jimenez, J. L.; Canagaratna, M. R. Formation of low volatility organic compounds and secondary organic aerosol from isoprene hydroxyhydroperoxide low-NO oxidation. *Environ. Sci. Technol.* **2015**, *49*, 10330−10339.
(22) Krechmer, J. E.; Pagonis, D.; Ziemann, P. J.; Jimenez, J. L. Quantification of gas-wall partitioning in Teflon environmental chambers using rapid bursts of low-volatility oxidized species generated in situ. *Environ. Sci. Technol.* **2016**, *50*, 5757−5765.
(23) Shair, F. H.; Heitner, K. L. Theoretical model for relating indoor pollutant concentrations to those outside. *Environ. Sci. Technol.* **1974**, *8*, 444−451.
(24) Arey, J.; Winer, A. M.; Atkinson, R.; Aschmann, S. M.; Long, W. D.; Morrison, C. L.; Olszyk, D. M. Terpenes emitted from agricultural species found in California's Central Valley. *J. Geophys. Res.* **1991**, *96*, 9329−9336.
(25) Jokinen, T.; Sipila, M.; Richters, S.; Kerminen, V.-M.; Paasonen, P.; Stratmann, F.; Worsnop, D.; Kulmala, M.; Ehn, M.; Herrmann, H.; Berndt, T. Rapid autoxidation forms highly oxidized RO_2 radicals in the atmosphere. *Angew. Chem., Int. Ed.* **2014**, *53*, 14596−14600.
(26) Warneke, C.; de Gouw, J. A.; Kuster, W. C.; Goldan, P. D.; Fall, R. Validation of atmospheric VOC measurements by proton-transfer-reaction mass spectrometry using a gas-chromatographic preseparation method. *Environ. Sci. Technol.* **2003**, *37*, 2494−2501.
(27) Donahue, N. M.; Robinson, A. L.; Stanier, C. O.; Pandis, S. N. Coupled partitioning, dilution, and chemical aging of volatile organics. *Environ. Sci. Technol.* **2006**, *40*, 2635−2643.
(28) Pankow, J. F.; Asher, W. E. SIMPOL.1: a simple group contribution method for predicting vapor pressures and enthalpies of vaporization of multifunctional organic compounds. *Atmos. Chem. Phys.* **2008**, *8*, 2773−2796.
(29) Raventos-Duran, T.; Camredon, M.; Valorso, R.; Mouchel-Vallon, C.; Aumont, B. Structure-activity relationships to estimate the effective Henry's law constants of organics of atmospheric interest. *Atmos. Chem. Phys.* **2010**, *10*, 7643−7654.
(30) Jokinen, T.; Berndt, T.; Makkonen, R.; Kerminen, V.; Junninen, H.; Paasonen, P.; Stratmann, F.; Herrmann, H.; Guenther, A. B.; Worsnop, D. R.; Kulmala, M.; Ehn, M.; Sipila, M. Production of extremely low volatile organic compounds from biogenic emissions: Measured yields and atmospheric implications. *Proc. Natl. Acad. Sci. U. S. A.* **2015**, *112*, 7123−7128.
(31) Andino, J. M.; Wallington, T. J.; Hurley, M. D.; Wayne, R. P. A classroom demonstration of aerosols from biogenic hydrocarbons. *J. Chem. Educ.* **2000**, *77*, 1584−1586.
(32) Vartiainen, E.; Kulmala, M.; Ruuskanen, T. M.; Taipale, R.; Rinne, J.; Vehkamaki, H. Formation and growth of indoor air aerosol particles as a result of *d*-limonene oxidation. *Atmos. Environ.* **2006**, *40*, 7882−7892.
(33) Claflin, M. S.; Krechmer, J. E.; Hu, W.; Jimenez, J. L.; Ziemann, P. J. Functional group composition of secondary organic aerosol formed from ozonolysis of α-pinene under high VOC and autoxidation conditions. *ACS Earth Space Chem.* **2018**, *2*, 1196−1210.
(34) Waring, M. S. Secondary organic aerosol formation by limonene ozonolysis: Parameterizing multi-generational chemistry in ozone- and residence time-limited indoor environments. *Atmos. Environ.* **2016**, *144*, 79−86.
(35) Atkinson, R.; Arey, J. Atmospheric degradation of volatile organic compounds. *Chem. Rev.* **2003**, *103*, 4605−4638.
(36) Xu, L.; Møller, K. H.; Crounse, J. D.; Otkjaer, R. V.; Kjaergaard, H. G.; Wennberg, P. O. Unimolecular reactions of peroxy radicals formed in the oxidation of α-pinene and β-pinene by hydroxyl radicals. *J. Phys. Chem. A* **2019**, *123*, 1661−1674.
(37) Travers, J.; Marsh, S.; Aldington, S.; Williams, M.; Shirtcliffe, P.; Pritchard, A.; Weatherall, M.; Beasley, R. Reference ranges for exhaled nitric oxide derived from a random community survey of adults. *Am. J. Respir. Crit. Care Med.* **2007**, *176*, 238−242.
(38) Zhou, S.; Young, C. J.; VandenBoer, T. C.; Kahan, T. F. Role of location, season, occupant activity, and chemistry in indoor ozone and nitrogen oxide mixing ratios. *Environ. Sci.: Process. Impacts* **2019**, *21*, 1374.

DOI: 10.1021/acs.estlett.9b00425
Environ. Sci. Technol. Lett. 2019, 6, 520−524